Generalized effective-medium approximation for particle transport: Random-trap model

J. W. Haus
Physics Department, Rensselaer Polytechnic Institute, Troy, New York 12180-3590

K. W. Kehr
Institut für Festkörperforschung, Forschungszentrum Jülich GmbH, D-5170 Jülich, Federal Republic of Germany

(Received 28 August 1990)

The effective-medium approximation for particle transport on lattices with random traps is generalized to include weighted initial conditions. It is argued that an inhomogeneous term must be included in the generalized master equation. We provide results for d-dimensional lattices with random traps and uniform bias fields. The effective-medium-approximation results in one and two dimensions are compared with numerical simulations for selected moments up to fourth order, and for the conditional probability distribution. Good agreement between theory and simulation is found; this confirms the necessity of including an inhomogeneous term and provides an accurate procedure for other models of transport in disordered media.

I. INTRODUCTION

This article will be devoted to the investigation of a generalized effective-medium approximation (GEMA) for hopping transport of particles in lattices with random site energies, commonly called random-trap models (RTM). We employ the effective-medium approximation to obtain an average description of transport in those random systems. A wealth of exact results is available for the RTM and other lattice models of disorder in one dimension, for reviews, see Refs. 1–3. In higher dimensions, exact results are scarce and hence approximations are needed. The main incentive of this work is the problem of the proper inclusion of the initial conditions, and the aim is to develop a *generalized* effective-medium approximation for a case where the initial conditions are important.

The typical effective-medium type averaging procedures use uniform initial conditions, i.e., the particle starts at each site with equal probability. If stationary states are used to describe the initial conditions, quite often the situation arises that the initial conditions are functions of the random transition rates. Hence the initial conditions are themselves random variables and they must be treated carefully in the averaging procedures. A case in point is the random-trap model where the transition rates out of a given site are random variables but are the same in each direction. The site occupancies in the stationary states are inversely proportional to the transition rates out of the sites. Another case is the random-barrier model (RBM) with a bias field in one direction. There is an increased probability of finding the particle sitting before a high barrier, as a consequence of the applied drift field. In this article we restrict our treatment to the RTM in a bias field in one and higher dimensions.

Without bias, the mean-square displacement of a particle in the RTM is a strictly linear function of time in all dimensions d when equilibrium initial conditions apply.[4] Further exact results for the moments of the displacement in the RTM without bias were obtained by Denteneer and Ernst[5] in $d=1$, 2, and 3. Exact results on the velocity autocorrelation function of the RTM, including bias were deduced in $d=1$ by Lehr, Machta, and Nelkin.[6]

The description of particle transport in disordered systems by an effective medium is usually made in the form of a generalized master equation. We will point out the necessity of introducing an inhomogeneous generalized master equation, in the generic case of nonuniform initial conditions. The inhomogeneous term can be derived by the projection-operator method[7,8] and we show that it is directly related to the initial conditions. Projection-operator methods were applied to the average description of particle transport in disordered lattices by Klafter and Silbey.[9] However, they omitted the inhomogeneous term in their derivations.

The projection-operator method gives the general structure of the resulting disorder-averaged master equation, it is not a practical method of explicitly performing the averages. A practical method of deriving disorder-averaged equations for conditional probabilities and related quantities is the effective-medium approximation.[10,11] Guided by the general results of the projection-operator method, in Ref. 12 a generalized effective-medium approximation was outlined where nonuniform initial conditions were incorporated in an inhomogeneous term. The procedure was then demonstrated on the RTM including bias fields. In this article a more detailed account of these derivations for the RTM will be given, including the comparison with numerical simulations of the RTM. We emphasize that the comparison with the numerical simulations is important to assess the validity of the approximations made in the effective-medium description. Our derivations will not be directly compared with real experiments. We will discuss, however, the general relation of our derivations to different types

of experiments with different initial conditions. This will be done in the conclusion.

There are other prototype models of lattices with disordered transition rates.[2] Each model has its own simplicities and difficulties, this pertains when drift is included. Hence we restrict the derivations in this article to the RTM including drift. A subsequent publication will address the random-barrier model.[13]

II. PROJECTION-OPERATOR RESULTS FOR THE GENERALIZED MASTER EQUATION

We first define the random-trap model to have a specific model as the basis for further discussions. The RTM is defined by a set of random transition rates $\{\Gamma_{\mathbf{n}}\}$ where $\Gamma_{\mathbf{n}}$ is the transition rate of a particle *from* the lattice site $\mathbf{n}$ to any of its neighbor sites. We consider d-dimensional cubic lattices of length L in each direction and $\mathbf{n}\in Z_L^d$ where Z_L is the set of integers $\{1,2,\ldots,L\}$. Without the introduction of a bias, the transition rates of the RTM possess site symmetry. We assume that the $\Gamma_{\mathbf{n}}$ are independently distributed and selected from a probability distribution $\rho(\Gamma)$. We further assume that all (also the inverse) moments of $\rho(\Gamma)$ exist.

The transport of a particle on this model, including bias, is described by the set of Markovian master equations,

$$\frac{dP(\mathbf{n},t;\mathbf{m},0)}{dt}=\sum_{\hat{\mathbf{e}}}[b_{-\hat{\mathbf{e}}}\Gamma_{\mathbf{n}+\hat{\mathbf{e}}}P(\mathbf{n}+\hat{\mathbf{e}},t;\mathbf{m},0) - b_{\hat{\mathbf{e}}}\Gamma_{\mathbf{n}}P(\mathbf{n},t;\mathbf{m},0)] , \tag{1}$$

where $P(\mathbf{n},t;\mathbf{m},0)$ is the conditional probability of the particle being at site $\mathbf{n}$ at time t, when it started at site $\mathbf{m}$ at time 0. The variable $\hat{\mathbf{e}}$ denotes the nearest-neighbor unit vectors. The bias field is parametrized by the variable $b_{\hat{\mathbf{e}}}$; for $b_{\hat{\mathbf{e}}}>1$, the transition rate increases in direction $\hat{\mathbf{e}}$; and for $b_{\hat{\mathbf{e}}}<1$ it decreases. We introduce the symmetry $b_{-\hat{\mathbf{e}}}=b_{\hat{\mathbf{e}}}^{-1}$.

If there is no bias, $b_{\hat{\mathbf{e}}}\equiv 1$, Eq. (1) has the steady-state solution given by

$$\rho_{\mathbf{n}}=\frac{1}{\Gamma_{\mathbf{n}}\sum_{\mathbf{n}}\Gamma_{\mathbf{n}}^{-1}} . \tag{2}$$

The sum extends over the $N=L^d$ lattice sites. If the lattice is large, then

$$\sum_{\mathbf{n}}\Gamma_{\mathbf{n}}^{-1}/N\rightarrow\langle\Gamma^{-1}\rangle , \tag{3}$$

where the angular brackets denote the average over all realizations of the random transition rates. The steady-state solution Eq. (2) is also valid for the case of bias, when periodic boundary conditions are imposed on the hypercubic lattice.

Of course, the set of master equations, Eq. (1), cannot be solved for a macroscopic lattice. One is interested in the average behavior of a particle, in different realizations of the random lattice. Hence equations for the disorder-averaged conditional probability are required. The projection-operator method provides a general scheme for the derivation of equations for disorder-averaged quantities. For a review of the projection-operator method, see Haake[7] or Grabert;[8] the application of this method to hopping transport of particles in disordered lattices was made by Klafter and Silbey.[9]

The projection-operator D for the problem of transport in disordered lattices is defined as the ensemble average over the set of disordered (quenched) transition rates. Applied to a quantity A, it is given by $DA=\langle A\rangle$. The projection onto the orthogonal space is denoted by $(I-D)$ where I is the unit operator. The master equation, Eq. (1), is symbolically written as

$$\frac{dP}{dt}=LP , \tag{4}$$

where P is a vector whose components are the conditional probabilities and L is a matrix containing the set of disordered transition rates. By application of standard procedures of the projection-operator method[7,12] the master equation can be brought into the form

$$\frac{d\langle P(t)\rangle}{dt}=\langle L\rangle\langle P(t)\rangle + \int_0^t dt' K(t-t')\langle P(t')\rangle+I(t) . \tag{5}$$

The kernel is given by the disorder average

$$K(t-t')=\langle L\exp[(I-D)L(t-t')](I-D)L\rangle , \tag{6}$$

and the inhomogeneous term is given by

$$I(t)=\langle L\exp[(I-D)Lt](I-D)P(0)\rangle . \tag{7}$$

It is evident from the derivation of the generalized master equation by the projection-operator technique that an inhomogeneous term is present in the general case; only when $(I-D)P(0)=0$, does the inhomogeneous term vanish. This is the case for uniform initial conditions which are equilibrium occupation probabilities, e.g., for the RBM without an external drift field. In the case of the random-trap model

$$IP(0)\neq DP(0) ;$$

when $P(0)$ is chosen in accordance with the stationary solution. This means when a specific site (say, $\mathbf{n}=\mathbf{0}$) is chosen as the initial one, its occupation is determined from the stationary solution. $IP(0)$ leaves the occupancy of a specific site unaltered while $DP(0)$ averages it out. We note that Klafter and Silbey[9] omitted the inhomogeneous term, although they refer to the model with randomly blocked sites where the initial conditions are certainly nonuniform. In this work it will be verified for the RTM that inclusion of the inhomogeneous term leads to consistent results for the appropriate conditional probabilities.

III. GENERALIZED EFFECTIVE-MEDIUM THEORY

A. The Green function

In this section we develop the effective-medium description of the RTM. This model is defined by a set of

transition rates $\{\Gamma_{\mathbf{n}}\}$. $\Gamma_{\mathbf{n}}$ is the transition rate from site $\mathbf{n}$ to any of its nearest-neighbor sites. Without bias, this model possesses a site symmetry that is depicted in Fig. 1(a) for $d=1$; namely, there is no tendency for the particle to jump toward or away from any of its neighbors. The addition of a bias field is shown in Fig. 1(b); the particle now tends to jump in a particular direction and migrates toward regions where the potential is lower.

The master equations governing this process are already presented and discussed in the previous section. For simplicity we restrict the derivations to the linear chain, square lattice, simple-cubic lattice, etc., but the procedure given below is general enough to be applied to other Bravais and non-Bravais lattices. We chose to bias the particle's migration along the x axis, i.e., $b_{\hat{\mathbf{x}}}=b>1$ and $b_{-\hat{\mathbf{x}}}=b^{-1}$, otherwise $b_{\hat{\mathbf{e}}}=1$ for $\hat{\mathbf{e}}\neq\hat{\mathbf{x}}$.

We take our ansatz for the systematic treatment of the averaged quantities from the results of Sec. II. The kernel $K(t-t')$ in Eq. (6) represents a time-dependent average transition probability; it is independent of the initial conditions. Only the inhomogeneous term, therefore, needs to be calculated using an appropriately weighted initial condition. To separate the task of calculating the average transition rate from the determination of the inhomogeneous term, we distinguish between two different quantities, that have different physical interpretations.[5,12] The Green function is calculated by averaging the conditional probability over the random rates with uniform initial conditions. On the other hand, we define the response function as the average of the conditional probability weighted by the initial conditions that correspond to the stationary state.

We stress that the initial conditions are important in calculating physical quantities; it is necessary therefore, to carefully define the averaged functions and distinguish between them in performing subsequent analyses.

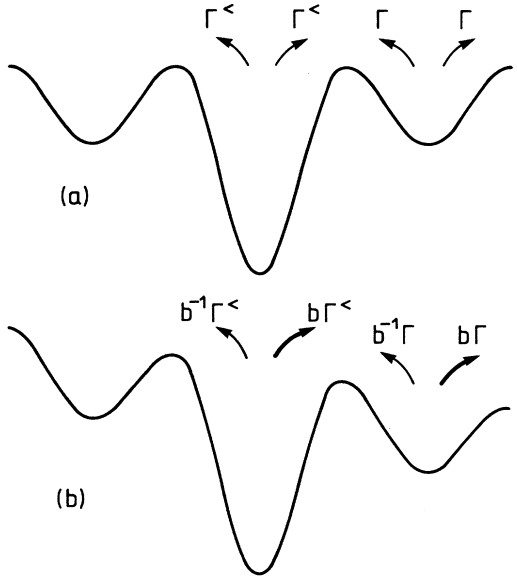

FIG. 1. Sketch of potential that would yield transition rates of the random-trap model by using an Arrhenius law. (a) Case of no bias. (b) Uniform bias to the right.

The first aim is to find a self-consistent expression for the average transition rate. This is performed by calculating the Green function. That is, we calculate the conditional probability when an average is taken over the ensemble of transition rates that are distributed over the lattice, $\langle P(\mathbf{n};t;\mathbf{m},0)\rangle$ and the initial conditions for the disorder-averaged conditional probability, or Green function, are the uniform occupation $P(\mathbf{n},0;\mathbf{m},0)=\delta_{\mathbf{nm}}$ for each realization of the set $\{\Gamma_{\mathbf{n}}\}$ on the lattice.

Since the Green function is calculated using uniform occupation of the lattice sites, the projection-operator method yields no inhomogeneous term in the averaged equation for $\langle P(\mathbf{n},t;\mathbf{m},0)\rangle$. Thus, it is sufficient to determine the effective transition rates self-consistently from the averaged conditional probability. The Green function is denoted as $G_{\mathbf{n}}(t)$ and it obeys the homogeneous generalized master equation. We assume that it is sufficient to restrict the time-dependent average transition rates to nearest-neighbor transitions. The generalized master equation has then the form

$$\frac{dG_{\mathbf{n}}(t)}{dt}=\int_0^t dt'\sum_{\hat{\mathbf{e}}}\Gamma(t-t')[b_{-\hat{\mathbf{e}}}G_{\mathbf{n}+\hat{\mathbf{e}}}(t')-b_{\hat{\mathbf{e}}}G_{\mathbf{n}}(t')], \tag{8}$$

with the memory kernel $\Gamma(t-t')$. This kernel represents the sum of the terms $\langle L\rangle$ and $K(t-t')$ of Eq. (5). The factors $b_{\hat{\mathbf{e}}}$ represent the overall bias which is explicitly given in Eq. (1). Equation (8) is entirely solved in the Fourier-Laplace domain for the space and time variables, respectively,

$$\tilde{G}(\mathbf{k},s)=[s+\tilde{\Gamma}(s)f(\mathbf{k},b)]^{-1}, \tag{9}$$

where the "form factor" $f(\mathbf{k},b)$ is given by

$$f(\mathbf{k},b)=2(d-1)+b+b^{-1}-b\exp(-ik_x)-b^{-1}\exp(ik_x)-2\sum_{\alpha\neq x}\cos k_\alpha . \tag{10}$$

The lattice constant has been taken as unity. Of course, the approximate memory kernel $\Gamma(t)$ or $\tilde{\Gamma}(s)$ must be determined self-consistently from a multiple-scattering formalism or an embedding procedure. The latter procedures are equivalent to approximations of the multiple-scattering expansions,[10] but their analysis is easier to realize.[11] We use the latter method.

We choose a cluster of sites in the lattice that have specified transition rates $\Gamma_{\mathbf{n}}$ taken from $\rho(\Gamma)$. This cluster is embedded into an effective medium composed of transition rates $\Gamma(t)$ between the nearest neighbors. The conditional probability for this medium with the cluster embedded in it will be designated by $P(\mathbf{n},t;\mathbf{m},0)$ and it also has the initial condition $P(\mathbf{n},t;\mathbf{m},0)=\delta_{\mathbf{nm}}$. For simplicity we introduce the notation $P(\mathbf{n},t)=P(\mathbf{n},t,\mathbf{o},0)$ in the rest of the article. The site $\mathbf{m}=\mathbf{o}$ is designated as the initial site, or origin.

For the RTM the transition rates from a site, $\mathbf{n}$, in the cluster to a site $\mathbf{n}'$ outside the cluster, will be the random transition rate Γ_n; on the other hand, the transition rate from site $\mathbf{n}'$ to $\mathbf{n}$ is $\Gamma(t)$. The master equations for the conditional probability are

$$\frac{dP(\mathbf{n},t)}{dt}=\sum_{\hat{\mathbf{e}}}\left[\int_0^t dt'\Gamma(t-t')[(1-\Delta_{\mathbf{n}+\hat{\mathbf{e}}})b_{-\hat{\mathbf{e}}}P(\mathbf{n}+\hat{\mathbf{e}},t')-(1-\Delta_{\mathbf{n}})b_{\hat{\mathbf{e}}}P(\mathbf{n},t')]\right.$$
$$\left.+\Delta_{\mathbf{n}+\hat{\mathbf{e}}}b_{-\hat{\mathbf{e}}}\Gamma_{\mathbf{n}+\hat{\mathbf{e}}}P(\mathbf{n}+\hat{\mathbf{e}},t)-\Delta_{\mathbf{n}}b_{\hat{\mathbf{e}}}\Gamma_{n}P(\mathbf{n},t)\right]. \tag{11}$$

$\Delta_{\mathbf{n}}$ is a variable that is nonzero for sites with random transition rates. We choose a single site cluster at $\mathbf{n}=\mathbf{o}$ hence $\Delta_{\mathbf{n}}=\delta_{\mathbf{n},\mathbf{o}}$.

It is convenient to write these equations in the form of a pure effective-medium term and a term with differences between the effective transition rate and the random transition rate. The extra terms are finite in number and they are treated as an inhomogeneity in the infinite set of integro-differential equations. These equations are solved by Fourier transforming the spatial coordinates and Laplace transforming the time variable; this leads to the result

$$\tilde{P}(\mathbf{k},s)=\tilde{G}(\mathbf{k},s)+\frac{\delta\tilde{\Gamma}(s)}{\tilde{\Gamma}(s)}[s\tilde{G}(\mathbf{k},s)-1]\tilde{P}(\mathbf{n}=\mathbf{o},s)\ , \tag{12}$$

where $\delta\tilde{\Gamma}(s)=\Gamma_{\mathbf{o}}-\tilde{\Gamma}(s)$. By inverse Fourier transformation an equation relating $\tilde{P}(\mathbf{n}=\mathbf{o},s)$ to $\tilde{G}_{\mathbf{o}}(s)$ is obtained:

$$\tilde{P}(\mathbf{n}=\mathbf{o},s)=\frac{\tilde{\Gamma}(s)\tilde{G}_{\mathbf{o}}(s)}{\tilde{\Gamma}(s)+\delta\tilde{\Gamma}(s)[1-s\tilde{G}_{\mathbf{o}}(s)]}\ . \tag{13}$$

The average is now taken over the random transition rate appearing in the embedded cluster. The condition is imposed that the average $\langle\tilde{P}(\mathbf{o},s)\rangle$ is identical with the lattice Green function $\tilde{G}_{\mathbf{o}}(s)$; this is the self-consistency condition that determines the function $\tilde{\Gamma}(s)$.

The result for the average transition rate is

$$0=\left\langle\frac{\delta\tilde{\Gamma}(s)}{\tilde{\Gamma}(s)+\delta\tilde{\Gamma}(s)[1-s\tilde{G}_{\mathbf{o}}(s)]}\right\rangle\ . \tag{14}$$

The ensuing transition rate is time dependent and is independent of the initial conditions chosen. Note that Eq. (14) has the same form as for the RBM. To proceed further, we require the response function.

B. The response function

We now consider the response function, $F(\mathbf{n},t)$, which includes the stationary initial conditions. To derive $F(\mathbf{n},t)$ we use again the method of embedding a cluster of sites (actually only one site) with specified transition rates into an effective medium. We determine a modified conditional probability $P'(\mathbf{n},t)$ using initial conditions which correspond to the stationary solution Eq. (2). Specifically,

$$P'(\mathbf{n}=\mathbf{o},0)=\frac{\overline{\Gamma}}{\Gamma_{\mathbf{o}}}\ , \tag{15}$$

where $\overline{\Gamma}$ is a short notation for $\langle\Gamma^{-1}\rangle^{-1}$. Note that the stationary solution is also applicable in the case of drift when periodic boundary conditions are employed. The equation obeyed by $\tilde{P}'(\mathbf{k},s)$ is similar to Eq. (12), with one term modified,

$$\tilde{P}'(\mathbf{k},s)=\tilde{G}(\mathbf{k},s)P'(\mathbf{n}=\mathbf{o},0)+\frac{\delta\tilde{\Gamma}(s)}{\tilde{\Gamma}(s)}[s\tilde{G}_{\mathbf{o}}(s)-1]\tilde{P}'(\mathbf{n}=\mathbf{o},s)\ . \tag{16}$$

The average of the conditional probability $\tilde{P}'(\mathbf{k},s)$ over the distribution $\rho(\Gamma_{\mathbf{o}})$ yields the response function $\tilde{F}(\mathbf{k},s)$. Equation (16) shows that the average of $\tilde{P}'(\mathbf{n}=\mathbf{o},s)$ over the disorder is required. This average can be evaluated along similar lines as indicated in the previous subsection, some algebra and the use of the self-consistency condition Eq. (14) are necessary. The final result is

$$\tilde{F}(\mathbf{k},s)=\frac{1+f(\mathbf{k},b)[\tilde{\Gamma}(s)-\overline{\Gamma}]/s}{s+\tilde{\Gamma}(s)f(\mathbf{k},b)}\ . \tag{17}$$

This equation is equivalent to an inhomogeneous master equation with the kernel $\tilde{K}(\mathbf{k},s)=\tilde{\Gamma}(s)f(\mathbf{k},b)$ and the inhomogeneity

$$I(\mathbf{k},s)=f(\mathbf{k},b)[\tilde{\Gamma}(s)-\overline{\Gamma}]/s\ . \tag{18}$$

The inhomogeneous term, in the site number representation is

$$\tilde{I}_{\mathbf{n}}(s)=\sum_{\hat{\mathbf{e}}}\{b_{\hat{\mathbf{e}}}\delta_{\mathbf{n},\mathbf{o}}-b_{-\hat{\mathbf{e}}}\delta_{\mathbf{n},\mathbf{n}+\hat{\mathbf{e}}}\}\frac{[\overline{\Gamma}-\tilde{\Gamma}(s)]}{s}\ . \tag{19}$$

This term is localized; it includes the initial state and its nearest neighbors. The consequences of the inhomogeneous term on the behavior of the response function will be apparent in the further sections.

C. Determination of the kernel

In later sections we want to give explicit results on the moments, and on the Green and response functions themselves. We thus need the kernel $\tilde{\Gamma}(s)$ of the effective-medium description, which is implicitly given by the self-consistency condition Eq. (14). It is, of course, not possible to completely solve for $\tilde{\Gamma}(s)$ because it is a complicated function depending explicitly on the Green function, which itself depends on $\tilde{\Gamma}(s)$. We have, therefore, expanded $\tilde{\Gamma}(s)$ in a small- and large-s expansion using the self-consistency condition Eq. (14). For large s we expand in powers of $1/s$,

$$\tilde{\Gamma}(s)=\langle\Gamma\rangle\left[1+\frac{\delta_1}{s}+\frac{\delta_2}{s^2}+\frac{\delta_3}{s^3}+\cdots\right]. \tag{20}$$

The average transition rate is

$$\langle\Gamma\rangle=\langle\Gamma_0\rangle\ ; \tag{21}$$

the next three corrections to this are

$$\delta_1=-\langle\delta\Gamma^2\rangle F/\langle\Gamma\rangle ,$$
$$\delta_2=\langle\delta\Gamma^3\rangle F^2/\langle\Gamma\rangle+\langle\delta\Gamma^2\rangle(2d+F^2) , \tag{22}$$
$$\delta_3=-F(2d^2\langle\delta\Gamma^2\rangle^2/\langle\Gamma\rangle+6d\langle\Gamma\rangle\langle\delta\Gamma^2\rangle+4d\langle\delta\Gamma^3\rangle)$$
$$-F^3(\langle\Gamma\rangle\langle\delta\Gamma^2\rangle+2\langle\delta\Gamma^3\rangle-\langle\delta\Gamma^2\rangle^2/\langle\Gamma\rangle$$
$$+\langle\delta\Gamma^4\rangle/\langle\Gamma\rangle) ,$$

where $\delta\Gamma=\Gamma_0-\langle\Gamma\rangle$ and the function F is given by

$$F=2(d-1)+b+b^{-1} . \tag{23}$$

The expansion for small s reads

$$\tilde{\Gamma}(s)=\bar{\Gamma}(1+\gamma_1 s+\gamma_2 s^2+\gamma_3 s^3+\cdots) . \tag{24}$$

The average jump rate at long times is $\bar{\Gamma}=\langle 1/\Gamma_0\rangle^{-1}$. Let

$$\kappa_n=\left\langle\left[1-\frac{\bar{\Gamma}}{\Gamma_0}\right]^n\right\rangle . \tag{25}$$

The next three corrections are then

$$\gamma_1=\kappa_2 G_1 ,$$
$$\gamma_2=\kappa_2^2 G_1^2+\kappa_2 G_2-\kappa_3 G_1^2 ,$$
$$\gamma_3=\tfrac{1}{2}\kappa_2 G_3+\kappa_2^2(G_1 G_2-2G_1^3)+\kappa_2^3 G_1^3 \tag{26}$$
$$-2\kappa_3 G_1 G_2-2\kappa_2\kappa_3 G_1^3+\kappa_4 G_1^3 .$$

The coefficients G_1,G_2,G_3 are related to the Green function without a bias and $\tilde{\Gamma}(s)\to\bar{\Gamma}$ and its derivatives evaluated at the values $s=\bar{\Gamma}(b+b^{-1}-2)$. They are given by

$$G_1=\tilde{G}_0(s),\quad G_2=\frac{d}{ds}\tilde{G}_0(s),\quad G_3=\frac{d^2}{ds^2}\tilde{G}_0(s) . \tag{27}$$

In one dimension, the Green function used in Eq. (27) is explicitly given by

$$\tilde{G}_o(s)=(s^2+4s\bar{\Gamma})^{-1/2} . \tag{28}$$

The coefficients G_1,G_2,G_3 are evaluated as

$$G_1=1/(\bar{\Gamma}|b-b^{-1}|) ,$$
$$G_2=-(b+b^{-1})/(\bar{\Gamma}^2|b-b^{-1}|^3) , \tag{29}$$
$$G_3=[(b+b^{-1})^2+2]/(\bar{\Gamma}^3|b-b^{-1}|^5) .$$

In two dimensions, the Green function without bias is given by an elliptic function,

$$\tilde{G}_0(s)=\frac{2}{\pi(s+4\bar{\Gamma})}K\left[\frac{4\bar{\Gamma}}{s+4\bar{\Gamma}}\right] . \tag{30}$$

For the definition of the elliptic function K, see Gradsteyn and Ryzhik (Ref. 14, p. 709). The elliptic function is related to the hypergeometric function by

$$K(z)=\frac{\pi}{2}\,{}_2F_1(\tfrac{1}{2},\tfrac{1}{2};1;z) .$$

This is exploited in our computation of the coefficients G_2 and G_3. The coefficients in Eq. (27) for $d=2$ are

$$G_1=\frac{2}{\pi F\bar{\Gamma}}K(\tfrac{4}{F}) ,$$
$$G_2=-\frac{G_1}{F\bar{\Gamma}}-\frac{{}_2F_1(\frac{1}{2},\frac{1}{2};2;\frac{4}{F})}{2\bar{\Gamma}^2F^2(F-4)} , \tag{31}$$
$$G_3=\frac{G_1}{\bar{\Gamma}^2F^2}-\frac{G_2}{\bar{\Gamma}F}+\frac{24\,{}_2F_1(\frac{1}{2},\frac{1}{2};2;\frac{4}{F})}{\bar{\Gamma}^3F^3(F-4)}$$
$$-\frac{36\,{}_2F_1(\frac{1}{2},\frac{1}{2};3;\frac{4}{F})}{\bar{\Gamma}^3F^3(F-4)^2} ,$$

where F is defined in Eq. (23) and we set $d=2$. These expressions are evaluated in Sec. V when we compare the GEMA to the Monte Carlo simulations.

We add a comment on the validity of the coefficients γ_i of the small-s expansion of the kernel $\tilde{\Gamma}(s)$. Lehr, Machta, and Nelkin[6] devised an exact expansion scheme for the calculation of the velocity autocorrelation function (VAF). The VAF is related to the second moment of the response function in the stationary situation, hence one may express the VAF in terms of the kernel $\tilde{\Gamma}(s)$ of the GEMA and insert the small-s expansion of $\tilde{\Gamma}(s)$. On the other hand, one may use the technique of Ref. 6 to derive the small-s expansion of the VAF exactly. Comparison of the exact expansion with the expansion based on the GEMA shows that the coefficients γ_1 and γ_2 are exact in $d=1$. We did not proceed to higher orders, nor did we compare the large-s expansions.

Finally, we note that the coefficients $\{\gamma_i\}$ diverge as $b\to 1$. The asymptotic terms at long time apply in a drift dominated time regime, i.e., $t>t_d=2(b+b^{-1})/(b-b^{-1})^2\bar{\Gamma}$ (Ref. 12). In the time regime between the short-time and drift dominant expansions, i.e., $1<\bar{\Gamma}t<\bar{\Gamma}t_d$, there is an intermediate time regime where algebraic terms, such as powers of $t^{1/2}$ in $d=1$ are important. For large bias, $\bar{\Gamma}t_d\approx 1$ and the intermediate regime is not observed, but for small bias, the long-time regime will not overlap with the short-time regime.

IV. NUMERICAL PROCEDURE

We use a Monte Carlo algorithm to simulate the diffusion of the particle on a disordered lattice. The regular lattice has a set of jump rates Γ, in the absence of bias. An ensemble of disordered lattices is prepared by distributing defect jump rates, $\Gamma^<$, randomly on the sites; these rates are smaller than the nondefect rates, $\Gamma^<<\Gamma$. Each lattice is prepared with a concentration, c, of defect jump rates. In all cases we chose $c=0.2$. The size of the defect jump rate is scaled to the jump rate Γ. For a nondefect site, when the particle attempts to jump, it will succeed with certainty. However, when the particle is on a defect site, it will succeed in making a transition only with probability $\Gamma^</\Gamma$, on the average. For our simulations in this article, we chose $\Gamma^<=0.1\Gamma$, hence, the particle succeeds on the average once for every ten attempts to leave a defect site.

The particles are randomly distributed on each lattice of the ensemble and the members are independently chosen at random. This procedure ensures that the underlying stochastic dynamics of the individual transitions

is Poissonian. The particles are noninteracting and several particles may occupy the same site. In general, however, the particles on each lattice have different environments, hence, an average over the disorder is simultaneously realized when the random walk average is taken.

The bias field is characterized by the parameter b. For $b=1$, no bias is applied. Along the axis of the applied field, the transition probability in the positive direction is $b/(b+b^{-1})$ and in the negative direction it is $b^{-1}/(b+b^{-1})$. The directions perpendicular to the field have equal probabilities of jumping in the positive or negative direction. The usual time unit in Monte Carlo simulations is the Monte Carlo step per particle (MCS/p). During one MCS/p each particle is called once, on the average. The transition rate from a regular site to any of the neighbor sites (explicit b factors excluded) is then given in units of inverse MCS/p by $\Gamma=[2(d-1)+b+b^{-1}](\mathrm{MCS/p})^{-1}$. This relation ensures that $\sum_{\hat{e}} b_{\hat{e}}\Gamma=1$.

In order to approximate equilibrium initial conditions, the ensemble is prepared by first letting each particle on the average take 1000, or more, jumps, according to the above algorithm. In one dimension, we have used 3000 members of the ensemble and 200 sites. In two dimensions the lattices are rectangular with dimensions 100×60. The long axis is in the bias direction and 1000 members of the ensemble were taken. We do not study $d=3$ in this article. In all cases the times were small enough that the periodic boundary conditions did not influence the statistical averages.

The random number generator was a modified version of R250 developed by Kirkpatrick and Stoll[15] and the runs were made on an IBM 3081/K64 and an IBM 3090/600. A typical run in one dimension, as discussed above, required about 20 min of CPU time.

V. MOMENTS AND CUMULANTS

A. Results of the GEMA in $d=1$

1. *Moments in $d=1$*

In this section we study the behavior of the moments and the cumulants of the Green and the response functions for short and long terms. We first present analytic results from the GEMA, then we compare them with the Monte Carlo simulations.

The nth moment of a quantity $\tilde{A}(k,s)$ is obtained for $d=1$ in the Laplace domain by

$$\langle x^n\rangle(s)=(-1)^n\frac{\partial^n}{\partial(ik)^n}\tilde{A}(k,s)\bigg|_{k=0} . \tag{32}$$

By this procedure, the first two moments of the Green function $\tilde{G}(k,s)$ are found as

$$\langle x\rangle(s)=(b-b^{-1})\tilde{\Gamma}(s)/s^2 , \tag{33}$$

$$\langle x^2\rangle(s)=(b+b^{-1})\tilde{\Gamma}(s)/s^2+2(b-b^{-1})^2\tilde{\Gamma}^2(s)/s^3 . \tag{34}$$

The first moment of the response function $\tilde{F}(k,s)$ is

$$\langle x\rangle(s)=(b-b^{-1})\overline{\Gamma}/s^2 . \tag{35}$$

This result leads immediately to a linear behavior of the mean displacement with time, for all times

$$\langle x\rangle(t)=(b-b^{-1})\overline{\Gamma}t . \tag{36}$$

We note that this is an exact result for initial conditions corresponding to a stationary state. Further remarks on the significance of the result will be made below.

The second, third, and fourth moments of the response function are

$$\langle x^2\rangle(s)=(b+b^{-1})\overline{\Gamma}/s^2+2(b-b^{-1})^2\overline{\Gamma}\tilde{\Gamma}(s)/s^3 , \tag{37}$$

$$\begin{aligned}\langle x^3\rangle(s)=&(b-b^{-1})\overline{\Gamma}/s^2\\&+6(b+b^{-1})(b-b^{-1})\overline{\Gamma}\tilde{\Gamma}(s)/s^3\\&+6(b-b^{-1})^3\overline{\Gamma}\tilde{\Gamma}(s)^2/s^4 ,\end{aligned} \tag{38}$$

$$\begin{aligned}\langle x^4\rangle(s)=&(b+b^{-1})\overline{\Gamma}/s^2\\&+[8(b-b^{-1})^2+6(b+b^{-1})^2]\overline{\Gamma}\tilde{\Gamma}(s)/s^3\\&+36(b-b^{-1})^2(b+b^{-1})\overline{\Gamma}\tilde{\Gamma}(s)^2/s^4\\&+24(b-b^{-1})^4\overline{\Gamma}\tilde{\Gamma}(s)^3/s^5 .\end{aligned} \tag{39}$$

The large-s and small-s expansions of $\tilde{\Gamma}(s)$ are inserted into these equations to obtain the short- and long-time properties predicted by the generalized effective-medium theory.

The predicted short-time behavior of the first two moments of the Green function in $d=1$ is

$$\langle x\rangle(t)=(b-b^{-1})\langle\Gamma\rangle f_1(t)+\cdots ,$$

where

$$f_1(t)=t+\delta_1\frac{t^2}{2}+\delta_2\frac{t^3}{6}+\delta_3\frac{t^4}{24} , \tag{40}$$

$$\langle x^2\rangle(t)=(b+b^{-1})\langle\Gamma\rangle f_1(t)+2(b-b^{-1})^2\langle\Gamma\rangle^2\times\left[\frac{t^2}{2}+\delta_1\frac{t^3}{3}+(2\delta_2+\delta_1^2)\frac{t^4}{24}\right]+\cdots . \tag{41}$$

The short-time behavior of the second to fourth moment of the response function according to the GEMA is

$$\langle x^2\rangle(t)=(b+b^{-1})\overline{\Gamma}t+2(b-b^{-1})^2\overline{\Gamma}\langle\Gamma\rangle f_2(t) ,$$

where

$$f_2(t)=\frac{t^2}{2}+\delta_1\frac{t^3}{6}+\delta_2\frac{t^4}{24}+\delta_3\frac{t^5}{120} , \tag{42}$$

$$\begin{aligned}\langle x^3\rangle(t)=&(b-b^{-1})\overline{\Gamma}t+6(b+b^{-1})(b-b^{-1})\overline{\Gamma}\langle\Gamma\rangle f_2(t)\\&+6(b-b^{-1})^3\overline{\Gamma}\langle\Gamma\rangle^2 f_3(t)+\cdots ,\end{aligned}$$

where

$$f_3(t)=\frac{t^3}{6}+\delta_1\frac{t^4}{12}+(2\delta_2+\delta_1^2)\frac{t^5}{120}\ , \tag{43}$$

$$\begin{aligned}\langle x^4\rangle(t)=&(b+b^{-1})\overline{\Gamma}t\\&+[8(b-b^{-1})^2+6(b+b^{-1})^2]\overline{\Gamma}\langle\Gamma\rangle f_2(t)\\&+36(b-b^{-1})^2(b+b^{-1})\overline{\Gamma}\langle\Gamma\rangle^2 f_3(t)\\&+24\overline{\Gamma}\langle\Gamma\rangle^3(b-b^{-1})^4\left[\frac{t^4}{24}+\delta_1\frac{t^5}{40}\right]+\cdots\ .\end{aligned} \tag{44}$$

The long-time behavior of the first two moments of the Green function in the GEMA is

$$\langle x\rangle(t)=(b-b^{-1})\overline{\Gamma}(t+\gamma_1)\ , \tag{45}$$

$$\langle x^2\rangle(t)=(b+b^{-1})\overline{\Gamma}(t+\gamma_1)+2(b-b^{-1})^2\times\overline{\Gamma}^2\left[\frac{t^2}{2}+2\gamma_1 t+2\gamma_2+\gamma_1^2\right]+\cdots\ . \tag{46}$$

Finally, the long-time behavior of the second, third, and fourth moments of the response function is

$$\langle x^2\rangle(t)=2(b-b^{-1})^2\overline{\Gamma}^2 g_1(t)+(b+b^{-1})\overline{\Gamma}t+\cdots\ ,$$

where

$$g_1(t)=\frac{t^2}{2}+\gamma_1 t+\gamma_2\ , \tag{47}$$

$$\begin{aligned}\langle x^3\rangle(t)=&(b-b^{-1})\overline{\Gamma}t+6(b+b^{-1})(b-b^{-1})\overline{\Gamma}^2 g_1(t)\\&+6(b-b^{-1})^3\overline{\Gamma}^3 g_2(t)+\cdots\ ,\end{aligned}$$

where

$$g_2(t)=\frac{t^3}{6}+\gamma_1 t^2+(\gamma_1^2+2\gamma_2)t+2\gamma_3+2\gamma_1\gamma_2\ , \tag{48}$$

$$\begin{aligned}\langle x^4\rangle=&(b+b^{-1})^4\overline{\Gamma}^4\left[\frac{t^4}{12}+\gamma_1 t^3+3(\gamma_2+\gamma_1^2)t^2+(6\gamma_3+12\gamma_1\gamma_2+2\gamma_1^3)t+6\gamma_4+6\gamma_2^2+12\gamma_1\gamma_3+6\gamma_1^2\gamma_2\right]\\&+36(b+b^{-1})(b-b^{-1})^2\overline{\Gamma}^3 g_2(t)+[8(b-b^{-1})^2+6(b+b^{-1})^2]\overline{\Gamma}^2 g_1(t)+\cdots\ .\end{aligned} \tag{49}$$

Some remarks seem in order. We noted already that the mean displacement equation (36) following from the response function is strictly linear in time while the one resulting from the Green function has corrections, cf. Eqs. (40) and (45). The Green function describes the average behavior for uniform initial conditions. In this situation a particle makes initially larger displacements, on the average, until the stationary situation is reached. The result equation (36) following from the response function is analogous to the result[4] that the average mean-square displacement of particles in the RTM without bias is strictly linear when equilibrium initial conditions apply. We point out that the inclusion of the inhomogeneous term was essential in arriving at the correct result equation (36). The result[4] for the mean-square displacement of particles in the RTM without bias is obtained from Eqs. (42) and (47) by setting $b=1$. The inverse of the minus-first moment of the transition rate, $\overline{\Gamma}$, also enters the *short*-time behavior of the response function, in contrast to the Green function, where only $\langle\Gamma\rangle$ appears. The presence of $\overline{\Gamma}$ is again a consequence of the stationary initial conditions.

2. *Cumulants in d=1*

It is also interesting to consider the long-time behavior of the cumulants of the displacements, in $d=1$, as predicted by the GEMA. We evaluated the cumulants of the displacements from the response function up to fourth order and obtained

$$\langle x^2\rangle_c=(b+b^{-1})\overline{\Gamma}t+2(b-b^{-1})^2\overline{\Gamma}^2(\gamma_1 t+\gamma_2)+\cdots\ , \tag{50}$$

$$\langle x^3\rangle_c(t)=(b-b^{-1})\overline{\Gamma}t+6(b-b^{-1})^3\overline{\Gamma}^3[(\gamma_1^2+\gamma_2)t+2\gamma_1\gamma_2+\gamma_3]+6(b+b^{-1})(b-b^{-1})\overline{\Gamma}^2(\gamma_1 t+\gamma_2)+\cdots\ , \tag{51}$$

$$\begin{aligned}\langle x^4\rangle_c(t)=&(b+b^{-1})\overline{\Gamma}t+12(b-b^{-1})^4\overline{\Gamma}^4[(2\gamma_1^3+6\gamma_1\gamma_2+2\gamma_3)t+5\gamma_2^2+6\gamma_2\gamma_1^2+12\gamma_1\gamma_3+6\gamma_4]\\&+36(b+b^{-1})(b-b^{-1})^2\overline{\Gamma}^3[(\gamma_1^2+\gamma_2)t+2\gamma_1\gamma_2+2\gamma_3]+[8(b-b^{-1})^2+6(b+b^{-1})^2]\overline{\Gamma}^2(\gamma_1 t+\gamma_2)+\cdots\ .\end{aligned} \tag{52}$$

The result shows that in the GEMA with a cluster of one site, the cumulants up to the fourth order are proportional to t, asymptotically. Since the moments of order n themselves are asymptotically proportional to t^n, this result suggests an asymptotically Gaussian form of the probability distribution. More precisely, the asymptotic behavior of the distribution of the random variable $(x-\langle x\rangle)/t^{1/2}$ is under discussion. The third-order cumulant $\langle x^3\rangle_c$ could scale with $t^{3/2}$ and the fourth-order cumulant with t^2. The results in Eqs. (51) and (52) indicate that these cumulants are proportional to t, hence they vanish in the limit $t\to\infty$ when divided with $\langle x^2\rangle_c^{3/2}$ or $\langle x^2\rangle_c^2$ respectively. This means that an asymptotically Gaussian distribution is predicted from the cumulants up to fourth order, within the GEMA. Of course, more is needed to establish such a behavior, namely, the study of higher-order cumulants and of the corrections to the single-site GEMA.

3. *Moments in higher dimensions*

Finally, we consider the moments of the Green and the response functions in higher dimensions. We restrict the derivations to $d=2$; this is sufficient to establish the general behavior. We assume a bias in the x direction and decompose the form factor $f(\mathbf{k},b)$ in Eq. (10) into

$$\begin{aligned} &f(\mathbf{k},b)=f_1(k_1,b)+f_2(k_2)\ ,\\ &f_1(k_1,b)=b+b^{-1}-b\exp(-ik_1)-b^{-1}\exp(ik_1)\ ,\\ &f_2(k_2)=2-\exp(-ik_2)-\exp(ik_2)\ . \end{aligned} \tag{53}$$

The expansion of the Green or the response function with respect to k_1 can be performed with arbitrary $f_2(k_2)$. Finally f_2 is zero since the expansion coefficients are evaluated at $\mathbf{k}=0$, cf. (32). Hence the moments $\langle x^n\rangle(s)$ have the same *form* as in $d=1$, i.e., Eqs. (33)–(35) and Eqs. (37)–(39) can be used for the moments of the displacement in the bias direction. Also the formula for the small- and large-time expansions of the moments given before can be used. It is important that now the correct δ_i, γ_i in $d=2$ are introduced. The generalization to higher dimensions is obvious, only the appropriate δ_i, γ_i are needed as new elements.

To obtain the moments of the displacement in the direction perpendicular to the bias, one expands the Green or response function with respect to k_2. One simply takes the expansion of $f_2(k_2)$ and puts finally $f_1=0$. This amounts to using the results for $d=1$ with the replacements $b=b^{-1}=1$. For convenience we list the moments of the response function for the perpendicular direction to the bias:

$$\begin{aligned} &\langle y\rangle(s)\equiv 0,\quad \langle y^2\rangle(s)=2\bar{\Gamma}/s^2\ ,\\ &\langle y^3\rangle(s)\equiv 0,\quad \langle y^4\rangle(s)=2\bar{\Gamma}/s^2+24\bar{\Gamma}\tilde{\Gamma}(s)/s^3\ . \end{aligned} \tag{54}$$

Again, the formulas obtained in $d=1$ for the short- and long-time expansions of the moments can be used with the substitution $b=b^{-1}=1$, but the coefficients γ_i, δ_i have to be taken for the d-dimensional case under study and these coefficients are evaluated with the actual value of $b\neq 1$.

One consequence of these derivations is that the result, Eq. (36), for the linear behavior of the mean displacement under stationary initial conditions is also valid in higher dimensions.

B. Numerical results

In this section the predictions of the GEMA for the moments and cumulants are compared with the numerical simulations. Figure 2 shows the first moment of the response function, for various values of the bias parameter b in $d=1$. This quantity represents the mean displacement of a particle for stationary initial conditions and it is linear in time, as predicted by Eq. (36), over the whole time range. Figure 3 gives the first moment of the Green function, for various b values, which represents the mean displacement of a particle for uniform initial conditions. Now the mean displacement is no longer linear at small times and the straight lines are the asymptotic results from Eq. (45). One recognizes good agreement between the simulations and the predictions of the GEMA. The predictions for the short-time behavior are only valid up to a few MCS/p. According to Eq. (45), the asymptotic long-time behavior consists of a linear term and a constant shift. Since γ_1 itself is proportional to $(b-b^{-1})^{-1}$, the constant term is the same for all b values, for given disorder. The predicted long-time behavior is only slowly approached for smaller bias. The reason for this will be discussed in connection with the

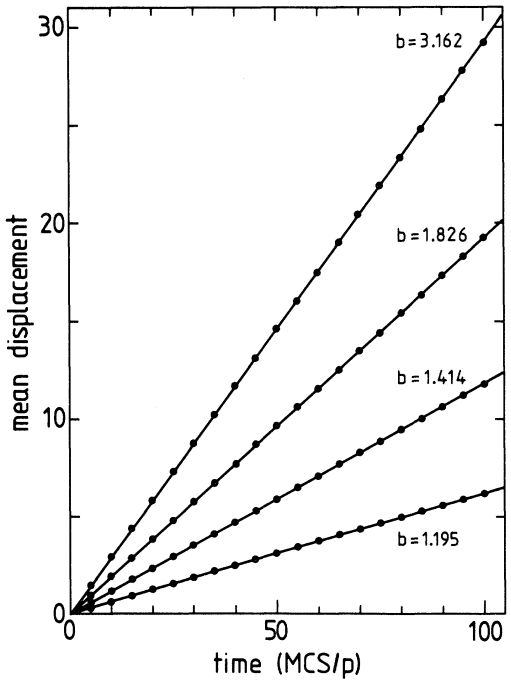

FIG. 2. First moment of the response function as a function of time, for different values of the bias. Lines, prediction of the GEMA; points, results of numerical simulations. The time unit is the Monte Carlo step per particle.

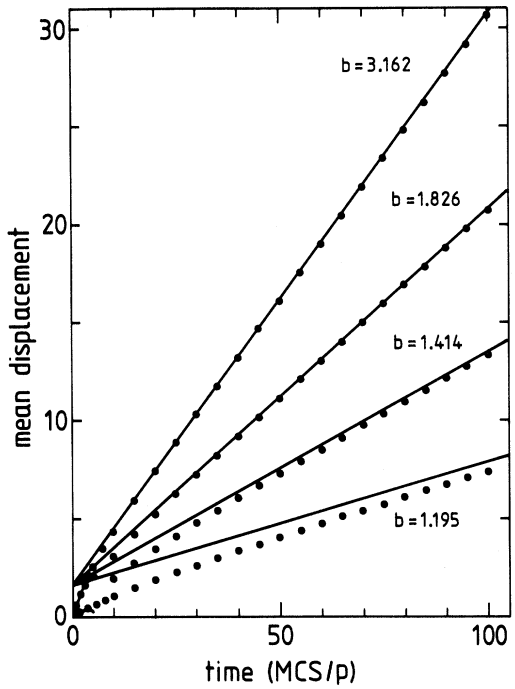

FIG. 3. First moment of the Green function as a function of time, for different values of the bias. Lines, short- and long-time expansions according to the GEMA. The short-time expansion is shown only for the smallest and largest bias value. Points, numerical results. Data points for short times and the intermediate bias values have been omitted for clarity.

second moment.

The second moment of the response function is shown in Fig. 4, for three values of the bias. One finds very good agreement between the simulations and the short- and long-time expansions at the largest bias value. For smaller b, the short-time expansion is still applicable over a considerable range (in the figure the short-time expansions were drawn up to times where they began to decrease). The long-time expansion is only slowly reached by the numerical data for the smallest bias.[12] This is due to the fact that the long-time expansion was made as a power series in t. When the bias is absent ($b=1$) the expansion has to be made in powers of $t^{1/2}$.[5] Inverse powers of $b-b^{-1}$ appear in the expansion terms of the series in t, rendering its convergence worse for smaller bias. The second moment of the Green function is represented in Fig. 5, for one smaller and one large value of the bias. The behavior is similar to the second moment of the response function, and the same arguments concerning the applicability of the long-time expansion can be made. The second moment of the Green function is larger than that of the response function, especially at smaller times. This is reasonable, because the particles make initially larger displacements when uniform initial conditions are imposed.

The third and the fourth moments of the response function are given in Figs. 6 and 7, respectively. The same general features are observed for these moments as for the second one. The small-time expansion provides a good description of the numerical data at small times. The long-time expansion agrees with the data for large bias, it is approached more slowly for smaller bias. As in the case of the second moment, the asymptotic behavior is not yet fully reached for the time shown in the figure.

The second cumulant of the response function is plotted in Fig. 8. This quantity represents the mean-square displacement of particles relative to their mean displacement, for equilibrium initial conditions. It should increase linearly with time, for large times. The figure shows good agreement between the simulations, with the exceptions as discussed above. The final asymptotic behavior is not yet fully reached in the figure. The third and the fourth cumulants of the response function was also determined from the simulations. The third cumu-

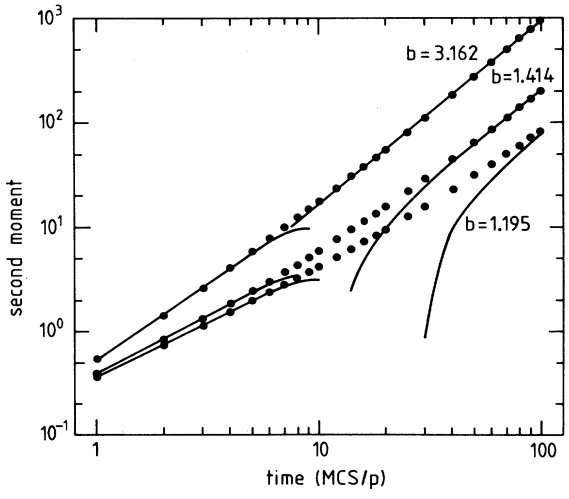

FIG. 4. Second moment of the response function as a function of time, for three values of the bias. Lines, short- and long-time expansions according to the GEMA. Points, numerical results.

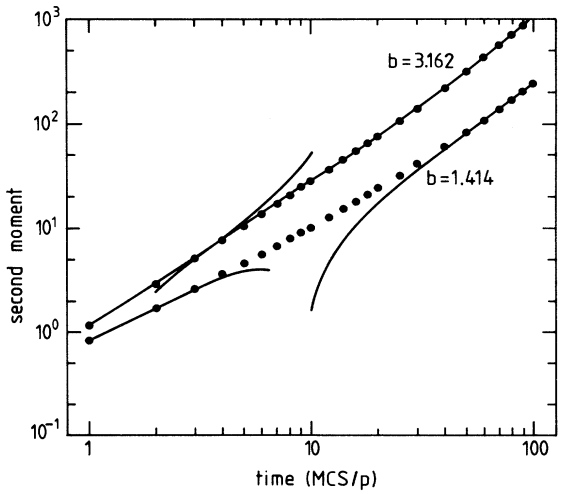

FIG. 5. Second moment of the Green function, as a function of time, for two values of the bias. Lines, short- and long-time expansions according to the GEMA. Points, numerical results.

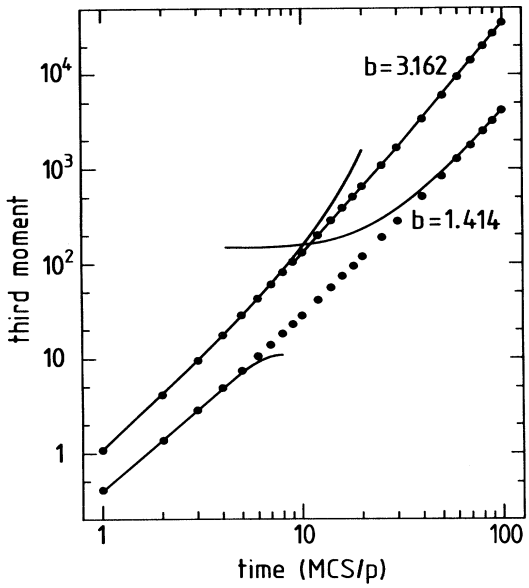

FIG. 6. Third moment of the response function as a function of time, for two values of the bias. Lines, short- and long-time expansions according to the GEMA. Points, numerical results.

lant exhibits the qualitative behavior that is predicted by the GEMA, however, there are quantitative discrepancies. The fourth cumulant could not be estimated from the simulations. In calculating the third, and, in particular, the fourth cumulant, differences of large numbers are taken. The statistics of our data was not sufficient to allow for a reliable determination of these two cumulants.

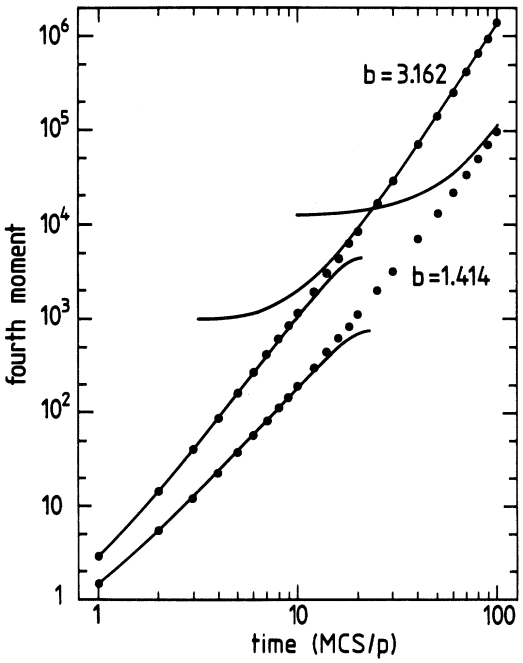

FIG. 7. Fourth moment of the response function as a function of time, for two values of the bias. Lines, short- and long-time expansions according to the GEMA. Points, numerical results.

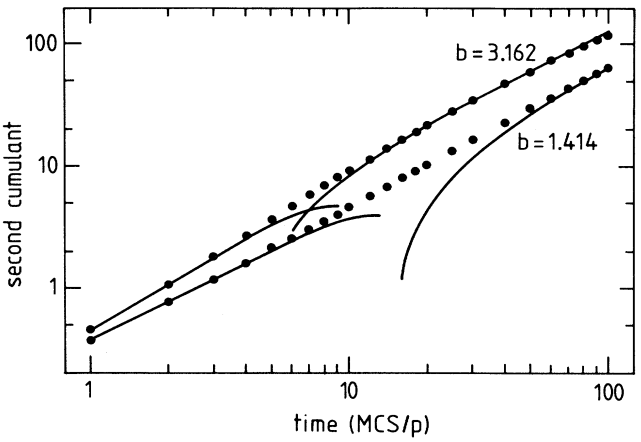

FIG. 8. Second cumulant of the response function as a function of time, for two values of the bias. Lines, short- and long-time expansions according to the GEMA. Points, numerical results.

In $d=2$ we display analogous results for the moments. The second moment of the response function in the longitudinal direction, i.e., the direction of the bias, is shown in Fig. 9(a) for three values of b. The short- and long-time asymptotic expansions, represented by the lines are calculated from Eqs. (42) and (47), respectively. The second moment transverse to the bias direction is plotted in Fig. 9(b) for two bias values, according to Eq. (54) this is a linear function of time. The simulation data agree to with 1% of the analytic result over the entire time range. It is interesting to note that, of course, the bias affects the value of $\overline{\Gamma}$, reducing the mean-square displacement, $\langle y^2 \rangle$, for larger bias values. In Fig. 9 the analytical results are in good agreement with the simulation data. The third and fourth moments of the response function in two dimensions are found in Figs. 10 and 11. Two large values for the bias were chosen. In Fig. 11 we use the fourth moment including the coordinate transverse to the bias direction, i.e., the contribution in Eq. (54) is included. Here the long-time asymptotic expansion does not overlap with the short-time expansion to cover the whole range. However, for times larger than 30, our long-time asymptotic results are in good agreement with the data.

We emphasize that in all comparisons between the GEMA and Monte Carlo simulations the corrections to order γ_3 and δ_3 were significant in obtaining the good agreement with the simulations.

VI. GREEN FUNCTION AND RESPONSE FUNCTION IN $d=1$

A. Representation of the kernel

In this subsection explicit results for the Green function $G_n(t)$ and the response function $F(n,t)$ in one dimension will be presented. The expression for $\tilde{G}(\mathbf{k},s)$ in Fourier and Laplace space was given in Eq. (9) and the one for $\tilde{F}(\mathbf{k},s)$ in Eq. (17). Both quantities contain the

kernel $\tilde{\Gamma}(s)$ and the form factor $f(\mathbf{k},b)$. While in principle the inverse Fourier transformation of $\tilde{G}(k,s)$ and $\tilde{F}(k,s)$ can be performed in $d=1$, the inverse Laplace transformation of these quantities cannot be done analytically because $\tilde{\Gamma}(s)$ is not known explicitly. Hence another approach is needed.

We have the small-s and large-s expansions of $\tilde{\Gamma}(s)$ and the coefficients are known up to $0(s^3)$ and $0(s^{-3})$, respectively, cf. Sec. III C. Bruenger, Peters, and Schulten[16] developed a representation of a function whose moments and inverse moments are known to some order, in terms of first-order rational approximants. To make the connection with their nomenclature, we write the expansions of $\tilde{\Gamma}(s)$ in the following way:

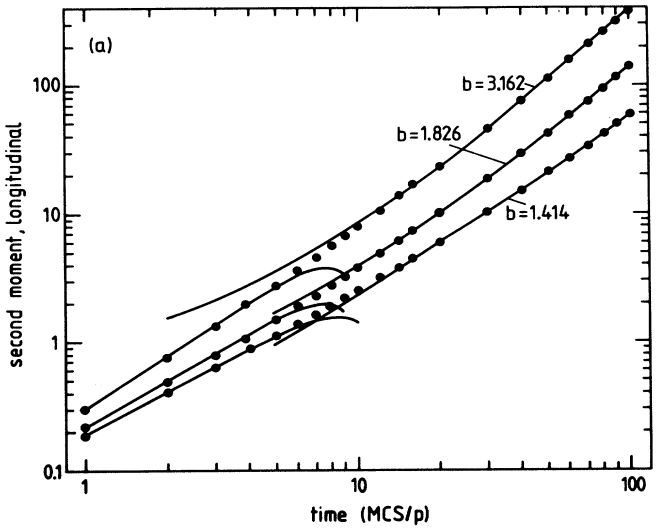

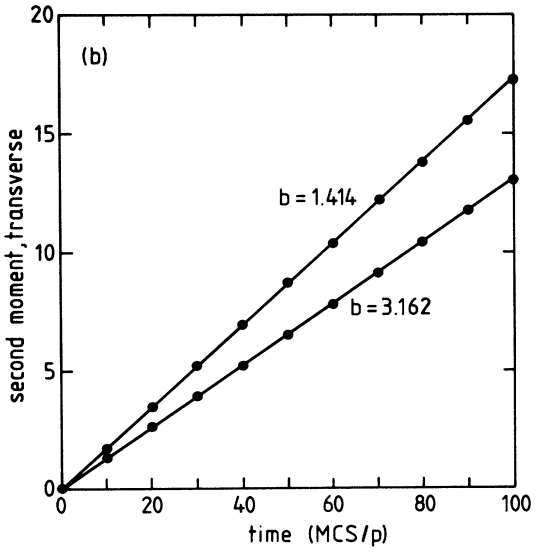

FIG. 9. The second moment of the response function in $d=2$, as a function of time. (a) The longitudinal moment, i.e., in the direction of the bias, is plotted for three values of the bias. (b) The moment is transverse to the direction of the applied bias. Lines, short- and long-time expansions according to the GEMA. Points, numerical results.

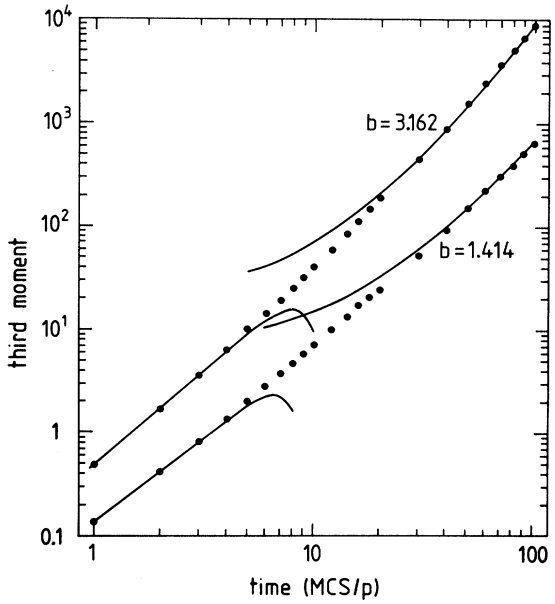

FIG. 10. Third moment of the response function in $d=2$ versus time. Lines, short- and long-time expansions according to the GEMA. Points, numerical results.

$$\tilde{\Gamma}(s)-\langle\Gamma\rangle \underset{s\to 0}{\to} \sum_{n=0}^{\infty} \mu_{-(n+1)}(-s)^n ,$$
$$\tilde{\Gamma}(s)-\langle\Gamma\rangle \underset{s\to \infty}{\to} \sum_{m=0}^{\infty} \mu_m(-s)^{-m} . \tag{55}$$

Comparison with Eqs. (21) and (24) gives

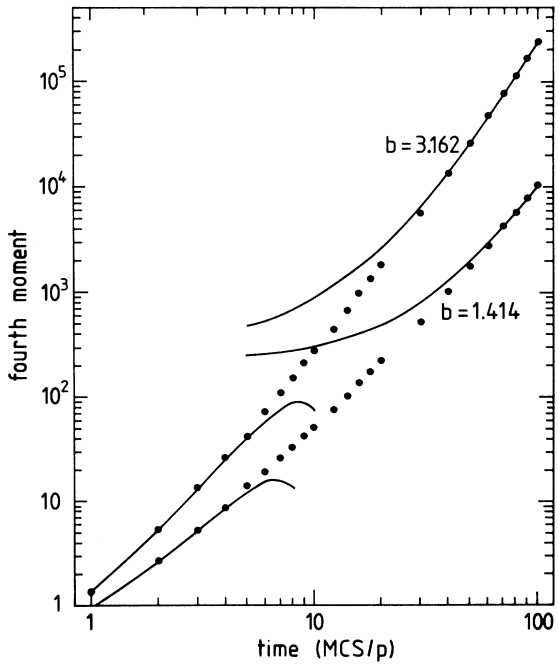

FIG. 11. The fourth moment of the response function in $d=2$ versus time. Lines, short- and long-time expansions according to the GEMA. Points, numerical results.

$$\mu_{-1}=\bar{\Gamma}-\Gamma\ ,$$
$$\mu_{-(n+1)}=(-1)^n\bar{\Gamma}\gamma_n,\quad n>0\ , \tag{56}$$
$$\mu_m=(-1)^m\langle\Gamma\rangle\delta_m,\quad m\geq 0\ .$$

The representation of $\tilde{\Gamma}(s)$ is

$$\tilde{\Gamma}(s)-\langle\Gamma\rangle=\sum_{i=1}^{r}\frac{a_i}{f_i+s}\ . \tag{57}$$

The papers[16,17] describe in detail how the amplitudes a_i and the frequencies f_i are determined from the μ_i. The index r indicates the order of the representation; an even number of moments/inverse moments is required. In addition, Bruenger, Peters, and Schulten developed a computer code to numerically calculate the coefficients a_i, f_i from the μ's. We used this code to derive the coefficients a_i, f_i up to $r=3$, from the sets $\{\delta_3,\ldots,\gamma_2\}$ or $\{\delta_2,\ldots,\gamma_3\}$, respectively, which were evaluated for given $\bar{\Gamma}$, $\langle\Gamma\rangle$, and b. To verify the quality of the representation equation (57) of the kernel, we solved numerically the self-consistency condition, Eq. (14), for given $\bar{\Gamma}$, $\langle\Gamma\rangle$, and b, for a wide range of s values. We found very good agreement [relative differences of $O(10^{-2})$ at most at intermediate s values]. Since we are more interested in the long-time properties of the quantities $F(n,t)$ and $G_n(t)$, we used always the set $\{\delta_2,\ldots,\gamma_3\}$ for the further calculations.

B. Comparison with simulations

We wish to compare the predictions of the GEMA for the Green function $G_n(t)$ and the response function $F(n,t)$ with the numerical simulations. To obtain $G_n(t)$ and $F(n,t)$ in the site number and time domain, we first make a numerical inverse Laplace transformation[18] of Eqs. (9) and (17) where we use the representation equation (57) of the kernel. We then Fourier transform the intermediate result to the site number representation by a fast-Fourier transform routine. Figures 12–14 give the results in the form of histograms for two different times and one value of the bias parameter b. The figures also contain the simulation results in the form of solid circles. One recognizes very good agreement between the predictions of the GEMA and the simulation results. The Green function which is derived for uniform initial conditions shows a rather smooth behavior as a function of the site number, see Figs. 12(a) and 13. Figure 13 is already suggestive of a spreading and drifting Gaussian distribution. The response function which is derived for stationary initial conditions has a large initial-site occupation probability, due to the larger occupation probability of a trap site. There is a second maximum of the distribution at site 10 for $t=100$ MCS; this number is somewhat smaller than the corresponding maximum of the Green function (site number 12).

We refrain from presenting additional figures of the

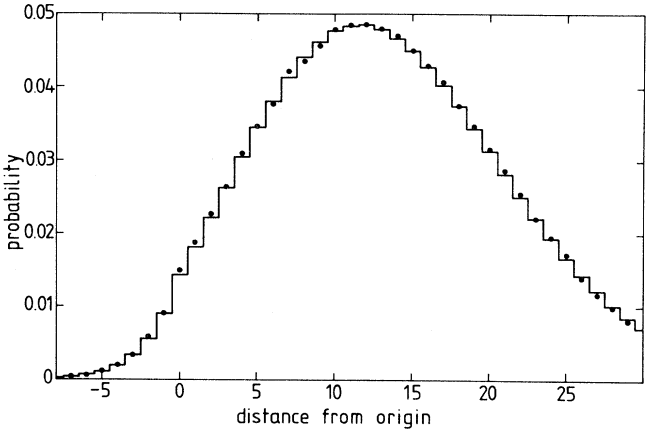

FIG. 13. Green function as a function of the distance from the initial position of particle, at the time $t=100$ MCS/p, for bias $b=1.414$. Histogram, results of the GEMA; points, numerical results.

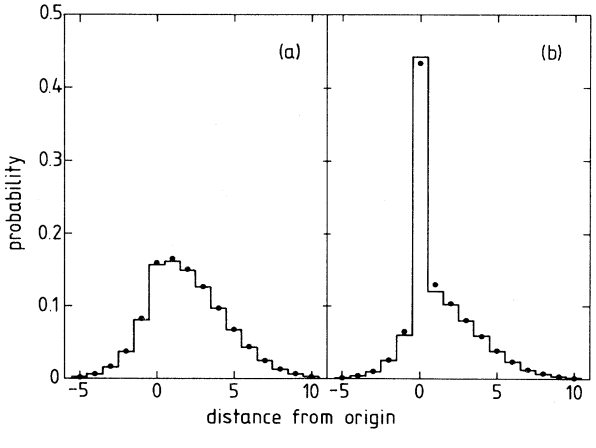

FIG. 12. Green function (a) and response function (b) as functions of the distance from the initial position of the particle, at the time $t=10$ MCS/p, for bias $b=1.414$. Histograms, results of the GEMA; points, numerical results.

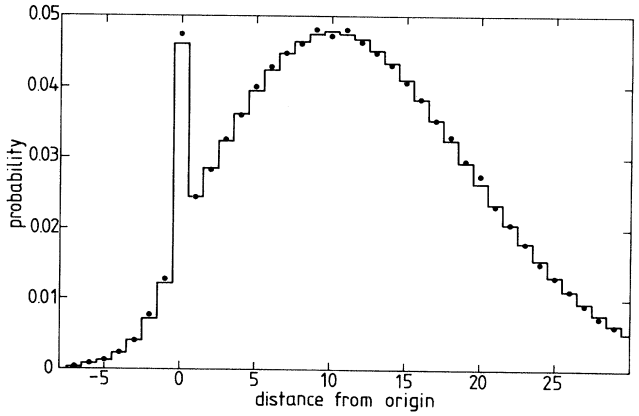

FIG. 14. Response function as a function of the distance from the initial position of particle, at the time $t=100$ MCS/p, for bias $b=1.414$. Histogram, results of the GEMA; points, numerical results.

Green and response functions for other values of the bias parameter or time; these quantities behave as expected from qualitative arguments. The figures shown are representative of the agreement between the GEMA predictions and the simulations, also for other parameter values. This is noticeable, since we made the approximation of a cluster of only one embedded site when we derived the self-consistency condition. As discussed before, the asymptotic behavior of the first and second moments is correctly obtained by this approximation. We now see that also the full distribution, at intermediate times and in the site number representation, is well predicted by the GEMA. It should be stressed that the correct behavior of the response function, including the enhanced occupancy of the initial site, follows from the inclusion of the inhomogeneous term Eq. (18) into the generalized master equation.

C. Initial-site occupation probability

It is instructive to consider the time dependence of the initial-site occupation probability separately. We shall consider this quantity for the response function, which is derived for stationary initial conditions. Equation (17) can be brought into the form

$$\tilde{F}(\mathbf{k},s)=G(\mathbf{k},s)+[1-sG(\mathbf{k},s)]\frac{\tilde{\Gamma}(s)-\bar{\Gamma}}{s\tilde{\Gamma}(s)} . \tag{58}$$

This equation is integrated over $\mathbf{k}$, in the first Brillouin zone. The result can be written as

$$\tilde{F}(\mathbf{o},s)=\{[\tilde{\Gamma}(s)-\bar{\Gamma}]/s+\bar{\Gamma}\tilde{G}_0(s)\}/\tilde{\Gamma}(s) . \tag{59}$$

The result holds for arbitrary dimensions d, but we will only consider $d=1$. Expansion of $\tilde{F}(o,s)$ for large s shows that the initial decay of $F(o,t)$ is determined by $\bar{\Gamma}$,

$$F(o,t)=1-\bar{\Gamma}(b+b^{-1})t+\cdots . \tag{60}$$

An initial decay with $\langle\Gamma\rangle$ is expected for the Green function $G_o(t)$. As seen below, the corrections to the initial-time behavior become important at relatively short times. A rough estimate of the long-time behavior can be obtained by expanding Eq. (59) for small s. A pole at

$$s=-\bar{\Gamma}\Big/\left[\frac{b+b^{-1}}{(b-b^{-1})^2}+\frac{\kappa_2}{b-b^{-1}}\right] \tag{61}$$

can be deduced, corresponding to exponential decay in the time domain. Since the Green function $\tilde{G}_o(s)$ contains a branch cut in $d=1$, the approximation of the small-s behavior of $\tilde{F}(o,s)$ by a single pole is not very satisfactory. Hence we made an inverse Laplace transform of Eq. (59) by a numerical routine.[18]

The result for $F(o,t)$ is plotted in Fig. 15 for several values of the bias parameter b, together with the results of the computer simulations. One recognizes very satisfactory agreement between the predictions of the GEMA and the simulations. The agreement seems to be somewhat better for the larger b values; this is because the drift terms become dominant more rapidly, as discussed in Ref. 12.

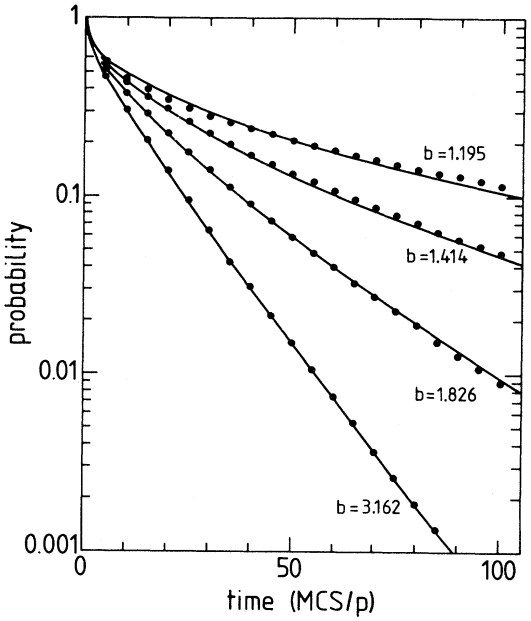

FIG. 15. Occupation probability of the initial site for stationary initial conditions as a function of time, for different bias values. Lines, prediction of the GEMA for the response function; points, numerical results.

VII. CONCLUSION

We have presented results from a generalized effective-medium theory for the random-trap model with uniform bias in one direction, and found good agreement with numerical simulations for this model. It was necessary to include an inhomogeneous term into the resulting generalized master equation, to properly deal with stationary initial conditions, where the site occpuancies are determined by the random transition rates. The inclusion of the inhomogeneous term leads to the correct behavior of the mean displacement of particles with time. Its inclusion was also instrumental in the derivation of the response function, which describes the probability of particle positions as a function of time for stationary initial conditions. Figure 14 demonstrates that the theory is corroborated by the numerical simulations. Of course, the experimental procedure determines which initial conditions are to be used in a real situation. For instance, if a photoconductivity experiment is made, where the charge carriers are uniformly created on a surface by a light pulse at the same time, uniform initial conditions on that surface would apply. On the other hand, when a neutron scattering experiment is made on a small concentration of hydrogen in metals, the hydrogen particles are thermalized, and equilibrium initial conditions apply. The Fourier transform of the *response function* would then yield the correct incoherent dynamical structure factor. Hence experiment does not provide a *general* rule whether the inhomogeneous term in the generalized master equation can be omitted. This depends on the specific situation, and the generic case is the one where it is present.

We comment on the relation to the continuous-time

random walk (CTRW) theory which is often used to describe transport in disordered media. In the CTRW theory the effect of the disordered medium is modeled by introducing generally time-dependent waiting-time distributions for the transitions of the particle. CTRW is equivalent to generalized master equations.[19] Our derivation shows that an inhomogeneous term is needed in the generalized master equation, hence also in the corresponding CTRW description. This conclusion is an extension of the previous argument of Tunaley[20] that the *first* transition of a particle must be treated differently in CTRW theory for equilibrium initial conditions. We did not compare our results with CTRW; such a comparison would yield "associated" waiting-time distributions in the sense of Ref. 21.

Another related phenomenon is "dispersive transport" which is often observed in amorphous semiconductors.[22,23] We find no indication for dispersive transport in our model. The numerical results suggest that the average transport of particles is described by spreading and moving Gaussian distributions for long times; the GEMA results for the cumulants up to fourth order support this assertion. Of course, these arguments do not constitute a proof. We point out that the absence of dispersive transport is asserted here for the random-trap model with transition rates where the moments and inverse moments exist. Apparently dispersive transport can be obtained for the random-trap model with transition rates where first inverse moment diverges. The general conditions under which dispersive transport does or does not occur, are not yet known. As already said in the Introduction, it is planned to extend these derivations to the case of the random-barrier model with a uniform bias field.[13]

ACKNOWLEDGMENTS

This work was supported by the NATO Collaborative Research Grant No. 850119. We thank R. Bittl and K. Schulten for providing us with the computer code described in Sec. VI A.

[1]G. H. Weiss and R. J. Rubin, Adv. Chem. Phys. **52**, 363 (1983).
[2]J. W. Haus and K. W. Kehr, Phys. Rep. **150**, 265 (1987).
[3]S. Havlin and D. Ben-Avraham, Adv. Phys. **36**, 695 (1987).
[4]J. W. Haus, K. W. Kehr, and J. Lyklema, Phys. Rev. B **25**, 2905 (1982).
[5]P. J. H. Denteneer and M. H. Ernst, Phys. Rev. B **29**, 1755 (1984).
[6]W. Lehr, J. Machta, and M. Nelkin, J. Stat. Phys. **36**, 15 (1984).
[7]F. Haake, Springer Tracts Mod. Phys. **66**, 98 (1973).
[8]H. Grabert, Springer Tracts Mod. Phys. **95**, 1 (1982).
[9]J. Klafter and R. Silbey, Phys. Rev. Lett. **44**, 55 (1980).
[10]S. Summerfield, Solid State Commun. **39**, 401 (1981); T. Odagaki and M. Lax, Phys. Rev. B **24**, 5284 (1981); I. Webman, Phys. Rev. Lett. **47**, 1496 (1981).
[11]J. W. Haus, K. W. Kehr, and K. Kitahara, Z. Phys. B **50**, 161 (1983); Phys. Rev. B **25**, 4918 (1982).
[12]J. W. Haus and K. W. Kehr, Phys. Rev. B **36**, 5639 (1987).
[13]J. W. Haus and K. W. Kehr (unpublished).
[14]I. S. Gradshteyn and I. M. Ryzhik, *Table of Integrals, Series and Products* (Academic, New York, 1980).
[15]S. Kirkpatrick and P. E. Stoll, J. Comput. Phys. **40**, 517 (1981).
[16]A. Bruenger, R. Peters, and K. Schulten, J. Chem. Phys. **82**, 2147 (1985).
[17]K. Schulten, A. Bruenger, W. Nadler, and Z. Schulten, in *Synergetics—From Microscopic to Macroscopic Order,* edited by E. Frehland, Springer Series in Synergetis Vol. 22 (Springer, Berlin, 1984), p. 80.
[18]G. Honig and U. Hirdes, J. Comput. Appl. Math. **10**, 113 (1984).
[19]V. M. Kenkre, E. W. Montroll, and M. F. Shlesinger, J. Stat. Phys. **9**, 45 (1973).
[20]J. K. E. Tunaley, Phys. Rev. Lett. **33**, 1037 (1974).
[21]J. W. Haus and K. W. Kehr, Phys. Rev. B **28**, 3573 (1983).
[22]E. W. Montroll and B. J. West, in *Fluctuation Phenomena,* edited by E. W. Montroll and J. L. Lebowitz (North-Holland, Amsterdam, 1979).
[23]See, e.g., H. Schnörer, D. Haarer, and A. Blumen, Phys. Rev. B **38**, 8097 (1988).